Mammalian HEMK1 Methylates Glutamine Residue of the GGQ Motif of Mitochondrial Release Factors

Qi Fang
RIKEN Cluster for Pioneering Research, RIKEN
Yusuke Kimura
The University of Tokyo
Tadahiro Shimazu
RIKEN Cluster for Pioneering Research, RIKEN
Takehiro Suzuki
RIKEN Center for Sustainable Resource Science
Naoshi Dohmae
RIKEN Center for Sustainable Resource Science
Shintaro Iwasaki
RIKEN Cluster for Pioneering Research, RIKEN
Yoichi Shinkai (yshinkai@riken.jp)
RIKEN Cluster for Pioneering Research, RIKEN

Research Article

Keywords: post-translational modification, glutamine methylation, translation, mitochondria

Posted Date: November 17th, 2021

DOI: https://doi.org/10.21203/rs.3.rs-1049003/v1

Version of Record: A version of this preprint was published at Scientific Reports on March 8th, 2022. See the published version at https://doi.org/10.1038/s41598-022-08061-y.

Abstract

Despite limited reports on glutamine methylation, methylated glutamine is found to be highly conserved in a "GGQ" motif in both prokaryotes and eukaryotes. In bacteria, glutamine methylation of peptide chain release factors 1/2 (RF1/2) by the enzyme PrmC is essential for translational termination and transcript recycling. Two PrmC homologs, HEMK1 and HEMK2, are found in mammals. In contrast to those of HEMK2, the biochemical properties and biological significance of HEMK1 remain largely unknown. In this study, we demonstrated that HEMK1 is an active methyltransferase for the glutamine residue of the GGQ motif of all four putative mitochondrial release factors (mtRFs)—MTRF1, MTRF1L, MRPL58, and MTRFR. In HEMK1-deficient HeLa cells, GGQ motif glutamine methylation was absent in all the mtRFs. We examined cell growth and mitochondrial properties, but disruption of the HEMK1 gene had no considerable impact on the overall cell growth, mtDNA copy number, and mitochondrial membrane potential. Furthermore, mitochondrial protein synthesis was not affected in HEMK1 KO cells. Our results suggest that HEMK1 mediates the GGQ methylation of all four mtRFs in human cells; however, this specific modification seems mostly dispensable in cell growth and mitochondrial protein homeostasis under standard culture conditions.

Introduction

Post-translational modification (PTM) of proteins causes significant diversification and enhancement of protein functions. Although protein methylation is a relatively new research field, its ability to regulate gene expression has attracted increasing attention [1]. A large number of studies have been conducted on the methylation of lysine and arginine residues owing to their specific roles in histone PTMs, which are highly relevant in chromatin regulation and gene expression [2,3]. Besides adenosine triphosphate (ATP), *S*-adenosylmethionine (SAM)—the donor of methyl moiety for protein methylation—is the second most widely used cosubstrate in biological processes, indicating that protein methylation is a pervasive biochemical event involved in a wide range of cellular processes [4,5].

Glutamine methylation, although rarely studied, is one of the essential protein modifications in prokaryotes [6]. The Gly-Gly-Gln (GGQ) motif of release factors (RF1 and RF2) is a remarkable substrate for glutamine methylation. Generally, at the end of translation, the stop codons in transcripts are read by RF1 (UAA and UAG) and RF2 (UAA and UGA). Subsequently, these factors cleave the nascent polypeptide chain from the last linked tRNA in the peptidyl transferase center (PTC) of the ribosome. The GGQ motif in RF1 and RF2 plays a critical role in orienting a water molecule and facilitating a nucleophilic attack on the carbonyl carbon of the ester bond between the tRNA and the attached polypeptide. Glutamine methylation driven by the N^5-glutamine methyltransferase (PrmC) at the GGQ motif in both bacterial RF1 and RF2 can stabilize the GGQ motif at the PTC through hydrophobic interactions, thus enhancing the polypeptide-releasing activity by about 5 fold and 20 fold, respectively [7-10]. Sequence and structural analyses revealed that PrmC is a typical seven-stranded β-sheet methyltransferase containing a GxGxG type SAM-binding motif and an Asn-Pro-Pro-Tyr (NPPY) glutamine/cystine-binding motif. Deletion of the

SAM-binding motif of PrmC causes a loss of methylation in both RF1 and RF2 and results in an impaired growth phenotype in rich medium and lethality in nutrient-depleted medium [6]. In the *E. coli* genome, the *prmC* gene is positioned immediately downstream of its substrate (*prfA* gene, encoding RF1), ensuring in-time methylation of bacterial RF1 [6].

PrmC evolved divergently beyond the prokaryotic lineage. It evolved into a homolog protein Mtq2 in archaea (archaeal PrmC), with a slight difference in the molecular basis. A recent study published by van Tran *et al.*[11] demonstrated that in *H. volcanii*, a PrmC homolog *Hvo*Mtq2 could methylate *Hvo*aRF1, with *Hov*aRF3 and GTP acting as cofactors. In addition, unlike the bacterial PrmC, *Hvo*Mtq2 forms a heterodimer with a protein called multifunctional methyltransferase subunit 112 (*Hvo*Trm112). Although this dimerization is not essential for the methyltransferase activity of *Hvo*Mtq2, the enzymatic activity of the *Hvo*Mtq2-*Hvo*Trm112 heterodimer is enhanced [11]. Similar to the phenotypes induced by *prmC* inactivation in bacteria, the deletion of the *HvoMtq2* gene also causes growth retardation in *H. volcanii*[11].

In eukaryotic cells, two PrmC homologs, HEMK1 (also known as MTQ1 or MPRMC) and HEMK2 (also known as MTQ2 or N6AMT1), are localized in the mitochondria and cytosol, respectively [12,13]. HEMK2 exhibits similar enzymatic properties as those of the archaeal *Hvo*Mtq2. It requires the protein TRM112 as a binding partner and the eukaryotic peptide chain release factor subunit 3 (eRF3) and GTP as cofactors for efficient methylation of the eukaryotic peptide chain release factor subunit 1 (eRF1) [14]. The deletion of *scMtq2*, an HEMK2 homolog, in *S. cerevisiae* yielded a strain with multiple defects, including growth retardation, cold-sensitivity, and hypersensitivity to translational fidelity drugs [12]. It has been reported that the loss of HEMK2 leads to early embryonic lethality in mice [15]. In contrast to bacterial PrmC, mammalian HEMK2 has a broader range of substrate-binding activity, as it can also catalyze the methylation of lysine residues and nucleotides [16-18].

Similarly, *sc*Mtq1, another PrmC homolog found in *S. cerevisiae*, can methylate the mitochondrial peptide chain release factor 1 (Mrf1), required for translation termination inside the organelle [19]. The loss of methylation in Mrf1 shows no significant impact when solid media is used, in contrast to the *PrmC* knockout (KO) phenotype in prokaryotes. The growth rate is about 15% slower when non-fermentable carbon sources are used in liquid media, suggesting that the methylation in Mrf1 affects mitochondrial function and energy metabolism [12]. Considering the high sequence identity of the enzyme and substrates, it is possible that the mammalian HEMK1 also possesses a methyltransferase activity against human mitochondrial peptide chain release factors (mtRFs). To date, four potential mtRFs have been identified in humans, namely MTRF1, MTRF1L, MRPL58 (also known as ICT1), and MTRFR (also known as C12orf65) [20-23]. As with other class I release factors, all four mtRFs contain the universally conserved GGQ motif. Although direct evidence from LC-MS/MS is missing, previous studies have demonstrated that HEMK1 could cause a 14 Da increase in molecular mass in a GGQ-containing peptide fragment derived from MTRF1L, implying the addition of a methyl group on the glutamine residue of the GGQ motif [13]. Recently, Desai *et al.* demonstrated that MTRFR is methylated at position Q73 in its GGQ motif [24]. Glutamine methylation on MTRF1 and MTRL58 has so far been reported yet. Furthermore, it

remains unclear how glutamine methylation of the GGQ motif affects the functions of mtRFs and mitochondrial translation. Thus, using proteomic analysis and genomic manipulation, we assessed the methyltransferase activity of HEMK1 towards the glutamine residue in GGQ motif of all potential mtRFs and examined possible biological consequences of HEMK1 depletion on mitochondrial properties.

Results

Domain and motif highlights of HEMK1 and mtRFs

Human HEMK1 is a 338 amino acid residue protein that shows high sequence and architecture similarity to bacterial PrmC (Figure 1A, 1B, and Figure S1). Similar to PrmC, HEMK1 belongs to the seven beta-strand class of methyltransferases. It possesses two distinct domains, a PrmC-N terminal domain (Pfam: PrmC_N, PF17827) and a methyltransferase small domain (Pfam: MTS, PF05175). The MTS domain contains a GxGxG type SAM-binding motif (position 117–121, referring to the bacterial PrmC sequence) and a NPPY glutamine/cystine-binding motif (position 183–186) (Figure 1B and Figure S1). Sequence-based algorithms, such as DeepMito, MitoFate, and DISOPRED, predicted that the first 40 residues of the HEMK1 N-terminal constitute a disordered, amphiphilic region containing a mitochondrial localization signal (MLS) (Figure S2A and Table S1), suggesting its localization in the mitochondria.

Amino acid sequence comparison of HEMK1 with another human Mtq2 homolog, HEMK2, revealed a radical amino acid replacement at the -1 position of the NPPY motif towards the N-terminus. At this position, a large and hydrophobic residue, phenylalanine, was found in HEMK2, yeast Mtq2, and *Hvo*PrmC *(Hvo*Mtq2*)*, but a small residue, serine/glycine, was found in HEMK1, yeast Mtq1, and PrmC (Figure 1B). Considering the critical role of the NPPY motif in the PrmC methyltransferase family [14], it is possible that HEMK1 and HEMK2 have different preferences for substrate binding.

Given the potential difference in substrate recognition, we thought that HEMK1 might modify GGQ-containing proteins other than eRF1 (targeted by HEMK2). The apparent candidates were four potential mtRFs—MTRF1, MTRF1L, MTPL58, and MTRFR [20-22]. All four mtRFs contained the conserved GGQ motif, while only MTRF1 and MTRF1L possessed a peptide chain release factor domain (Pfam: PCRF, PF03462) (Figure 1C and D). Permutation array of enzyme-substrate binding, using the sequence of eRF1 (position 179–192), revealed that G-Q-X3-R was the minimal recognition element for HEMK2, with the +4 position of the GGQ motif (R189) being absolutely essential [16] (Figure S2B). However, the arginine residue was not found at the +4 position of the GGQ motif in any of the four human mtRFs (Figure S2B and Figure S3), suggesting it is unlikely that HEMK2 is the methyltransferase responsible for human mtRFs.

HEMK1 is responsible for glutamine methylation of mtRFs

In order to determine whether HEMK1 methylates the mtRFs, we first confirmed the subcellular localization of both exogenously expressed enzymes and substrates. We co-expressed HA-tagged mtRFs individually with FLAG-tagged HEMK1 and performed immunofluorescence imaging to track their

localization. As expected and consistent with previous findings [13], HEMK1 and all four mtRFs were localized in the mitochondria (Figure 2A).

The purified recombinant PrmC could induce the methylation of bacterial RF1 *in vitro*[7]. Therefore, we attempted to detect the catalytic activity of recombinant HEMK1 against mtRFs *in vitro*; however, we did not observe any methyltransferase activity (data not shown). Hence, we decided to monitor the methyltransferase activity of HEMK1 in cells. We generated *HEMK1* KO HeLa cells via CRISPR-Cas9-mediated gene deletion. This deletion removed both the SAM-binding and substrate-binding motifs of HEMK1, resulting in a non-functional enzyme (Figure S4). To monitor the impact of HEMK1 depletion on the methylation of mtRFs, we expressed HA-tagged mtRFs individually in the naïve or *HEMK1*-KO HeLa cells and immune-purified the proteins for mass spectrometry analysis to detect methylated peptides. In naïve HeLa cells, we found glutamine methylation at Q252 of MTRF1L, Q313 of MTRF1, Q90 of MRPL58, and Q73 of MTRFR, within their GGQ motifs (Figure 2B, 2C, and Table S2). In contrast, these glutamine methylation events were not detected in the *HEMK1* KO cells (Figure 2B and Figure S5A). Exogenous expression of HEMK1-cFLAG in the *HEMK1* KO cells rescued and in fact enhanced the methylation of all four mtRFs, compared to that in the naïve cells (Figure 2B and Figure S5A).

To further clarify whether glutamine methylation of mtRFs is directly caused by the enzymatic activity of HEMK1, we generated a mutant HEMK1 with a Y242E substitution at the NPPY substrate-binding motif, which was predicted to inactivate the enzymatic activity. HEMK1^{Y242E} displayed the same mitochondrial localization as the wild-type HEMK1 (Figure S5B). However, the glutamine methylation of MTRF1L in *HEMK1* KO HeLa cells was not induced by the HEMK1^{Y242E} mutant (Figure S5A). These data further support that HEMK1 is a glutamine methyltransferase for all the four mtRFs.

Loss of *HEMK1* has minimal impact on HeLa cell physiology

Since the loss of PrmC in K-12 *E. coli* causes growth retardation [6], we assessed the impact of loss of *HEMK1* on cell growth. Under standard culture conditions, we monitored the growth of naïve and *HEMK1* KO HeLa cells, but did not find a clear difference between them (Figure 3A).

We then examined the impact of HEMK1 depletion on mitochondrial properties. Potential changes in two mitochondrial outer membrane proteins, VDAC1 and TOM22, and one mitochondrial inner membrane protein, COXIV, were investigated. However, the western blot analysis of these mitochondrial proteins revealed no changes in protein expression in *HEMK1* KO cells (Figure 3B).

It has been shown that mitochondria DNA (mtDNA) replication is a highly dynamic process that is linked to mitochondrial properties [25]. Therefore, we examined the impact of HEMK1 depletion on mtDNA copy number. To this end, we performed quantitative polymerase chain reaction using total DNA extracts to assess mtDNA (as a ratio to genomic DNA [gDNA]). Again, we failed to detect an apparent difference between naïve and *HEMK1* KO cells in terms of the mtDNA-gDNA ratios, which suggested that the mtDNA replication is likely not affected by HEMK1-mediated glutamine methylation on mtRFs (Figure 3C).

Additionally, we measured mitochondrial membrane potential via a flow cytometry-based assay. Here, we used MitoTracker Red, a membrane potential sensitive dye [26]. To control the effect of mitochondrial volume, we used membrane potential insensitive MitoTracker Green, which stains the mitochondrial membrane. Loss of *HEMK1* did not affect the signals of MitoTracker Red nor MitoTracker Green (Figure 3D). Thus, the impact on the net mitochondrial membrane potential (*i.e.*, MitoTracker Red normalized by MitoTracker Green) was marginal (Figure 3D).

HEMK1-mediated mtRF methylation could be dispensable in mitochondrial translation under standard culture conditions

Even with the limited physiological influence of HEMK1 depletion in mitochondria, we extended our analysis to mitochondrial translation. The mtDNA-encoded proteins are often excessively synthesized [27]; hence, conventional assays, such as western blotting, which measure steady-state protein levels, may not accurately reflect the impact of translation on *HEMK1* KO cells. To directly examine the impact of HEMK1 depletion and the role of HEMK1-mediated mtRFs methylation in mitochondrial translation, we performed fluorescent noncanonical amino acid tagging for mitochondrial translation (mito-FUNCAT) [28,29] to assess nascent protein synthesis in *HEMK1* KO cells. Out of four *HEMK1* KO clones, only KO clone #1 showed a decrease in nascent protein synthesis (Figure 4A, 4B, and Figure S6A), suggesting that this reduction stemmed from clonal variation and not HEMK1 depletion. To further ascertain this, we performed a rescue experiment using the wild-type HEMK1 and the HEMK1^{Y242E} mutant. As expected, the exogenous expression of neither wild-type HEMK1 nor HEMK1^{Y242E} mutant could reverse the changes in nascent protein synthesis in *HEMK1* KO clone #1 (Figure 4C, 4D, and Figure S6B). Furthermore, we performed western blot of an mtDNA-encoding protein MT-CO1. Similar to that in the mito-FUNCAT assay, *HEMK1* KO clone #1 showed lower MT-CO1 levels, and this phenotype was unrelated to *HEMK1* expression (Figure S7). Therefore, we concluded that HEMK1 depletion does not have a clear impact on mitochondrial translation.

Discussion

Ishizawa *et al.* reported HEMK1-mediated methylation (14 Da addition) of the MTRF1L-derived peptide [13]; here, we extended their findings onto other mtRFs and demonstrated that HEMK1 could methylate glutamine in the GGQ motif of all the four mtRFs. However, our analysis, which utilized exogenously expressed mtRFs, posed an analytic hurdle in the assessment of the methylation level of endogenous mtRFs. Given that the exogenously expressed mtRFs in naïve HeLa cells were methylated at a low frequency (Figure 2B and Figure S5A), the expression levels of HEMK1 in HeLa cells might be insufficient for full methylation of endogenous mtRFs. Additionally, even though the exogenously expressed HEMK1 could significantly enhance the methylation of mtRFs, the highest methylation level remained under 50%. One possibility for the incomplete methylation of mtRFs is that although HEMK1 is the enzyme responsible for glutamine methylation, other cofactor(s) may be needed for the catalytic reaction, as seen

in HEMK2 homologs [14]. Therefore, even if a sufficient amount of HEMK1 was exogenously supplied, the amount of such putative endogenous cofactor(s) might restrict this enzymatic reaction in our system.

Given that the loss of *PrmC* in *E. coli* K-12 strain leads to growth retardation [6,7,30], it is possible that the loss of methylation of mtRFs could cause similar biological consequences. Unfortunately, we could not identify any clear mitochondria-associated phenotypes in terms of cell growth, mitochondrial DNA replication, membrane potential, or even mitochondrial translation, a biological reaction directly supported by mtRFs. Methylated bacterial RFs can just accelerate the termination reaction, and this methylation is not essential at the termination step, as hydrolysis still occurs, although at a slower rate [9]. Again, the lower rate of mtRF methylation seen in HeLa cells suggests the limited role of mtRFs in mitochondrial protein synthesis. The restricted function of GGQ methylation in mtRFs is also supported by the Genome Aggregation Database [31], which shows the probability of "being the loss-of-function intolerant" score of *HEMK1* as 0, suggesting that *HEMK1* is unlikely an essential gene.

Although our results showed that HEMK1 depletion plays a limited role in translation, further analysis is required for clarifying any biological role of HEMK1-mediated GGQ methylation, especially a comprehensive molecular understanding of the four putative mtRFs, which has been long contested. mtRF1L is a canonical release factor with peptidyl-tRNA hydrolysis activity in ribosomes [22]. Furthermore, such activity has also been reported in MRPL58 (ICT1) [32], but the role in termination is still a matter of debate [33,34]. A recent structural study showed that MRPL58 recognizes the vacant A site in ribosomes translating truncated mRNA [23], suggesting that MRPL58 may rescue the stalled ribosomes on the ends of aberrant mRNAs, rather than participate in the standard termination reaction on stop codons. Moreover, Ramakrishnan and colleagues reported that MTRFR, associated with a split large subunit of the mitoribosome, serves as a quality control factor and cleaves the peptidyl-tRNAs halted in the middle of elongation [24]. In addition to termination and ribosome recycling, MRPL58 may also plays an important role in mitoribosome biogenesis or basal stability, as this protein is an integral constituent of the large subunit of the mitoribosome [20,35,36]. Further functional analysis of mtRFs in mitochondrial translation will help in enhancing the understanding of HEMK1-mediated methylation.

Materials And Methods

Cell culture

HeLa cells were obtained from RIKEN BioResource Research Center (BRC) and cultured in standard Dulbecco's modified Eagle' medium (DMEM high-glucose 4.5 g/l, Nacalai) with 10% FBS (Biosera), 1x glutamine (Gibco), and 1x Penicillin-Streptomycin (Gibco) at 37°C humidified incubators with 5% CO_2 supplied. The medium was changed routinely every 48 h. For the cell counting experiment, 0.5 million cells were seeded on a 10-cm dish for cell counting experiment. Cell counts started the next day after seeding for five consecutive days.

Sequence alignment, structure analysis, and phylogenetic analysis

Amino acid sequences were retrieved from UniProt (https://www.uniprot.org/). Alignments were generated using ClustalOmega (https://www.ebi.ac.uk/Tools/msa/clustalo/) with default settings. Alignments editing, color-coding, and phylogenetic analysis (by BLOUSUM62 matrix) were performed using the Jalview program. Domain organizations were retrieved from Pfam [37] database (http://pfam.xfam.org/). HEMK1/2 sequence-specific substrate binding sites were generated by WebLogo (http://weblogo.threeplusone.com/) [38]. DeepMito, deep-learning approaches trained with dataset comprising known mitochondrial proteins, (http://busca.biocomp.unibo.it/deepmito/) [39] and MitoFates, amino acid composition and physiochemical properties-based analysis, (http://mitf.cbrc.jp/MitoFates/cgi-bin/top.cgi) [40] were used for predictions of mitochondrial targeting sequences. Disordered region and secondary structure prediction were conducted using PSIPRED (http://bioinf.cs.ucl.ac.uk/psipred/) [41]. Sequence alignments with secondary structure elements were generated by ESPript (http://espript.ibcp.fr/ESPript/ESPript/) [42]. All UniProt protein IDs used in this study are listed in Table S1.

DNA construction and establishment of *HEMK1* KO cells

HEMK1 KO cell lines were generated by CRISPR-Cas9 mediated gene knockout. In brief, two sgRNAs (targeting *HEMK1* exon 5 and exon 8) were cloned into pL-CRISPR.EFS.tRFP (Addgene #57819) [43] and pKLV2-U6gRNA5(BbsI)-PGKpuro2ABFP-W (Addgene #67974) [44], respectively. After verification by Sanger sequencings, naïve HeLa cells were transfected with both sgRNA containing plasmids by Lipofectamine 2000 (Thermo Fisher Scientific) as instructed by the manufacturer. At 48 h post-transfection, HeLa cells were sorted by flow cytometry for RFP and BFP dual positive populations. Generally, 200-300 cells were seeded onto a 6-cm dish and cultured until visible colonies were seen. Single clones were then expanded in a 24-well dish. *HEMK1* KO clones were confirmed by PCR. For *HEMK1* KO clone #3 and #4, Sanger sequencing was also performed because large genomic deletion was only found on one allele. See Table S1 for the sequencing results.

DNA fragments encoding four mtRFs were PCR-amplified from HeLa total cDNA using specific primers. DNA fragments encoding mtRFs were cloned into EcoRI-linearized pQCXIP vector (Clontech) by In-Fusion cloning (Clontech) with HA tag at the C-terminal of mtRFs. DNA fragment encoding *HEMK1* cDNA was PCR-amplified from HeLa total cDNA by specific primers, and the PCR fragments was cloned into pcDNA3-cFLAG (Thermo Fisher Scientific) using EcoRI and NotI double digestion. *HEMK1* mutant was generated by site-directed mutagenesis with Phusion polymerase (Thermo Fisher Scientific). For transient expression (HEMK1, HEMK1^{Y242E}, and mtRF1L), HeLa cells were transfected using Lipofectamine 2000 (Thermo Fisher Scientific) followed the protocol from the manufacturer. At 72 h post-transfection, cells were harvested with ice-cold PBS, and then lysed in RIPA buffer for SDS-PAGE analysis.

Stable cell line establishment

HEMK1 wild-type and the mutants were subcloned from pcDNA3-cFLAG (Thermo Fisher Scientific) constructs into EcoRI-linearized pQCXIN (Clontech) by In-Fusion cloning (Clontech). Viral particles were

produced in HEK293T cells (cultured at the same conditions as HeLa cells) by pQCXIN/P and the Retroviral Expression System (Clontech). The medium was replaced on the next day after transfection. Viral particles were collected at 48 h post-transfection and filtered by 0.45-μm membrane (EMD). HeLa cells were infected by the viral particles (with 8 μg/ml polybrene, Sigma). At 24 h post-infection, cells were selected with neomycin (500 μg/ml for up to 14 d). Stable cell lines expressing mtRFs were generated similarly using the former established *HEMK1* wild-type/mutants cell lines (selected with 2 μg/ml puromycin for 3 d). Primers and vectors used in this study were listed in Table S1.

Western blot analysis

Cells harvested using ice-cold PBS (with 1x protease inhibitor cocktail [Nacalai] and 1 mM PMSF), were lysed by RIPA buffer (with 1x protease inhibitor cocktail [Nacalai] and 1 mM PMSF) on ice for 5 min. Sonication was performed on ice subsequently. The lysate was centrifuged at 10,000 *g,* 4°C for 10 min. The supernatant was transferred to a new tube, and protein concentration was measured using the Bradford Protein Assay Kit (BioRad Laboratories). The lysate was denatured by NuPAGE LDS Sample Buffer (Thermo Fisher Scientific) with 1 mM 2-mercaptoethanol at room temperature. Proteins were separated by SDS-PAGE and transferred onto PVDF membrane (Immobilon-FL-PVDF, Millipore). For imaging, both X-ray film (FUJIFILM) with chemiluminescence and ODYSSEY CLx (LI-COR Biosciences) with infrared fluorescence were used. In brief, PVDF membrane was blocked using TBS-T (1x TBS and 0.1% Tween-20) with skimmed milk at room temperature for 1 h, followed by incubation with the primary antibody in TBS-T with 3% BSA at 4°C overnight with mild shaking. The membrane was washed with TBS-T for 10 min twice before secondary antibody incubation. In the case when infrared fluorescence was used for detection, Tween-20 was omitted from the blocking buffer, and secondary antibody was used in the dark for 1 h at room temperature. Antibodies used in this study are listed in Table S1. Original blot images used for figures are shown in Figure S8.

Immunofluorescence microscopy analysis

HeLa cells were grown on 0.1% gelatin-coated cover glasses. Cells were first washed with PBS then fixed using 4% PFA room temperature for 10 min. Cells were washed with PBS twice, followed by permeabilization using PBS with 0.5% Triton X-100. Then, cells were blocked with 3% BSA in TBS-T at room temperature for 2 h. Primary antibodies and secondary antibodies were administered as guided by manufacturers. MitoTracker Red CMXRos reagent (Thermo Fisher Scientific) was added directly into the media at 30 min before PFA fixation for mitochondria staining. Slides were mounted on slide glasses (Matsunami) with Prolong with DAPI mounting reagent (Thermo Fisher Scientific). Images were captured and processed by Olympus FV3000 system and its suite software. Antibodies used in this study are listed in Table S1.

Detection of mitochondrial mass and membrane potential by flow cytometry

Cells (naïve HeLa, *HEMK1* KO clone #1, and *HEMK1* KO clone #2) were seeded on 6-cm dishes at 70% confluency one day before the analysis. On the day of analysis, cells were first washed with PBS once

and then replaced with Mitotracker Red CMXRos (200 nM) and Mitotracker Green FM (150 nM) containing PBS with 5% FCS. Cells were incubated at 37°C for 25 min. Then, cells were dissociated from the dishes by 0.5% Trypsin and neutralized by PBS with 5%FCS. Cells were pelleted and resuspended in 0.3 ml of PBS with 5%FCS for flow cytometry analysis.

Immunoprecipitation for mass spectrometry (MS) analysis

Stable mtRFs and mtRFs with HEMK1 (co-)overexpressing cells were first lysed on ice for 10 min using lysis buffer A (50 mM Hepes pH 7.5, 140 mM KCl, 10% glycerol, 0.5% NP40, 1x protease inhibitor cocktail [Nacalai], and 1 mM PMSF). The lysate was then sonicated with Ultrasonic Disruptor (TOMY UR-21P) with 70% output for 10 pluses on ice and precleared using Protein G Sepharose 4 Fast Flow beads (GE Healthcare) at 4°C for 30 min with mild rotation. The supernatant was collected by 10,000 *g* spinning at 4°C for 10 min and subsequently incubated with anti-HA antibody at 4°C for 1 h and then with Protein G beads for 2 h. Then, beads were collected at 500 *g* centrifugation and washed once with lysis buffer A and three times with bead wash buffer (20 mM Tris 6.8, 150 mM NaCl, 10% glycerol, and 1 mM PMSF). The beads were boiled in 1x Laemmli buffer at 95°C for 5 min for elution. Eluted proteins were separated on 15% Tris-glycine gel with MOPS buffer. Gels were stained using the Pierce Silver Stain for Mass Spectrometry kit (Thermo Fisher Scientific), and regions corresponding to different mtRFs were excised for mass spectrometry.

MS analysis

The excised gels were destained as instructed by the manufacturer. The proteins were digested in gel with trypsin (TPCK-treated, Worthington Biochemical Corporation). The peptide mixture was separated on a nanoflow LC (Easy nLC 1200; Thermo Fisher Scientific, Waltham, MA) using a nano-spray column (NTCC analytical column, C18, φ75 μm × 150 mm, 3 μm, Nikkyo Technos) with a linear gradient of 0–100% buffer B (80% aqueous acetonitrile containing 0.1% formic acid) at a flow rate of 300 nl/min over 20 min. The elution was sprayed online to a Q Exactive HF-X mass spectrometer (Thermo Fisher Scientific) equipped with a nano-spray ion source. The MS/MS data were acquired in a Top10 data-dependent manner. Proteins were identified using Proteome Discoverer 2.2 (Thermo Fisher Scientific) with MASCOT program 2.6 (Matrix science) using an in-house database. The mass spectra and mass chromatograms were drawn by Qual Browser 4.1.50 (Thermo Fisher Scientific).

qPCR analysis

MT-ND2 and ALU repeats were selected for quantification of mtDNA and gDNA content respectively. Total DNA was extracted with the Nucleospin DNA isolation kit (Macherey Nagel). One nanogram of total DNA was used for qPCR with Power SYBR Green PCR master mix (Thermo Fisher Scientific). Step one plus real-time PCR (Applied Biosystems) was performed according to the manufacturer's instruction. Data were processed and plotted with Microsoft Excel. For primers used in qPCR, see Table S1.

On-gel mito-FUNCAT assay

Cells (naïve HeLa, *HEMK1* KO clone #1, clone #2, and *HEMK1* KO clone #1 rescued lines) were grown on 6-well dish in standard culture media (-antibiotics) until the day of assay. Cells were washed with protein labelling media (DMEM [ThermoFisher Scientific], 10% FBS, 48 mg/ml L-cystine dihydrochloride [Nacalai], and 862 mg/ml L-alanyl-L-glutamine [Nacalai]) once and then incubated in methionine-free medium with L-homopropargylglycine 50 μM (Jena Bioscience) and anisomycin 100 μg/ml (Alomone Labs) for 4 h at 37°C humidified incubators with 5% CO_2 supplied. Cells were lysed with ice-chilled lysis buffer (20 mM Tris-HCl pH 7.5, 150 mM NaCl, 5 mM $MgCl_2$, 1% Triton X-100). Lysates were cleared by centrifugation for 10 min at 20,000 *g*, 4°C. The supernatants were used for CLICK reaction with Click-iT Cell Reaction Buffer Kit (ThermoFisher Scientific) and IRdye800CW Azide (LI-COR Biosciences), according to the manufacturer's instruction. After the CLICK reaction, free IRdye800CW Azide was removed using illustra MicroSpin G-25 Column (GE Healthcare) equilibrated with lysis buffer containing 1mM DTT. Samples were denatured at 50°C with 4x Protein Loading Buffer (LI-COR Biosciences) with 10% 2-mercaptoethanol (Nacalai). Samples were loaded onto the polyacrylamide gel (NuPAGE, 4 to 12%, Bis-Tris [ThermoFisher Scientific]) with 5 μl protein ladder marker (NIPPON Genetics). Electrophoresis was conducted in 1x MES buffer (ThermoFisher Scientific) for 22 min at 200 V constant. The gel was fixed with fixation reagent (40% ethanol, 10% acetic acid, and 50% ddH_2O) for 15 min at room temperature. After fixation, the gel was destained with MilliQ water and subsequently imaged by Odyssey CLx (LI-COR Biosciences) with IR800 channel for the newly synthesized mitochondrial polypeptides. For the total protein imaging, the same gel (after IR800-channel imaging) was incubated with GelCode Blue reagent (ThermoFisher) for 15-60 min then destained with MilliQ water. The destained gel was imaged by Odyssey CLx (LI-COR Biosciences) with IR700 channel. Original gel images used for figures were shown in Figure S8.

Declarations

ACKNOWLEDGEMENT

We thank the staff of the Support Unit for Bio-Material Analysis (BMA) at RIKEN Center for Brain Science (CBS) Research Resources Division (RRD) for DNA sequencing and flow cytometry. We are also grateful to Mingming Chen and Hironori Saito for technical helps. This study used the following materials: pL-CRISPR.EFS.tRFP from Benjamin Ebert and pKLV2-U6gRNA5(Bbsl)-PGKpuro2ABFP from Kosuke Yusa. We would also like to thank our colleagues at Shinkai laboratory and members of Iwasaki laboratory for their support and valuable comments.

FUNDING

This work was supported by a RIKEN internal research fund for Y.S. QF was funded by the International Program Associate (IPA) Fellowship and an International Joint Graduate School Program of RIKEN. S.I. was supported by the Ministry of Education, Culture, Sports, Science and Technology (MEXT) (a Grant-in-Aid for Transformative Research Areas [B], JP20H05784), the Japan Society for the Promotion of Science (JSPS) (a Grant-in-Aid for Young Scientists [A], JP17H04998; a Challenging Research [Exploratory], JP19K22406), the Japan Agency for Medical Research and Development (AMED) (AMED-CREST,

JP21gm1410001), and RIKEN (Pioneering Projects "Biology of Intracellular Environments" and Ageing Project). Y.K. was supported by a Grant-in-Aid for JSPS Fellows (JP20J10665) from JSPS. Y.K. was a RIKEN Junior Research Associate Program recipient and a JSPS Research Fellow (DC2).

References

1 Murn, J. & Shi, Y. The winding path of protein methylation research: milestones and new frontiers. *Nat Rev Mol Cell Biol***18**, 517-527, doi:10.1038/nrm.2017.35 (2017).

2 Ng, S. S., Yue, W. W., Oppermann, U. & Klose, R. J. Dynamic protein methylation in chromatin biology. *Cellular and molecular life sciences : CMLS***66**, 407-422, doi:10.1007/s00018-008-8303-z (2009).

3 Bedford, M. T. & Clarke, S. G. Protein arginine methylation in mammals: who, what, and why. *Molecular cell***33**, 1-13, doi:10.1016/j.molcel.2008.12.013 (2009).

4 Fontecave, M., Atta, M. & Mulliez, E. S-adenosylmethionine: nothing goes to waste. *Trends in biochemical sciences***29**, 243-249, doi:10.1016/j.tibs.2004.03.007 (2004).

5 Biggar, K. K. & Li, S. S. Non-histone protein methylation as a regulator of cellular signalling and function. *Nat Rev Mol Cell Biol***16**, 5-17, doi:10.1038/nrm3915 (2015).

6 Heurgue-Hamard, V., Champ, S., Engstrom, A., Ehrenberg, M. & Buckingham, R. H. The hemK gene in Escherichia coli encodes the N(5)-glutamine methyltransferase that modifies peptide release factors. *The EMBO journal***21**, 769-778, doi:10.1093/emboj/21.4.769 (2002).

7 Graille, M. *et al.* Molecular basis for bacterial class I release factor methylation by PrmC. *Molecular cell***20**, 917-927, doi:10.1016/j.molcel.2005.10.025 (2005).

8 Pierson, W. E. *et al.* Uniformity of Peptide Release Is Maintained by Methylation of Release Factors. *Cell reports***17**, 11-18, doi:10.1016/j.celrep.2016.08.085 (2016).

9 Zeng, F. & Jin, H. Conformation of methylated GGQ in the Peptidyl Transferase Center during Translation Termination. *Scientific reports***8**, 2349, doi:10.1038/s41598-018-20107-8 (2018).

10 Nakahigashi, K. *et al.* HemK, a class of protein methyl transferase with similarity to DNA methyl transferases, methylates polypeptide chain release factors, and hemK knockout induces defects in translational termination. *Proceedings of the National Academy of Sciences of the United States of America***99**, 1473-1478, doi:10.1073/pnas.032488499 (2002).

11 van Tran, N. *et al.* Evolutionary insights into Trm112-methyltransferase holoenzymes involved in translation between archaea and eukaryotes. *Nucleic acids research***46**, 8483-8499, doi:10.1093/nar/gky638 (2018).

12 Polevoda, B., Span, L. & Sherman, F. The yeast translation release factors Mrf1p and Sup45p (eRF1) are methylated, respectively, by the methyltransferases Mtq1p and Mtq2p. *The Journal of biological chemistry***281**, 2562-2571, doi:10.1074/jbc.M507651200 (2006).

13 Ishizawa, T., Nozaki, Y., Ueda, T. & Takeuchi, N. The human mitochondrial translation release factor HMRF1L is methylated in the GGQ motif by the methyltransferase HMPrmC. *Biochemical and biophysical research communications***373**, 99-103, doi:10.1016/j.bbrc.2008.05.176 (2008).

14 Liger, D. *et al.* Mechanism of activation of methyltransferases involved in translation by the Trm112 'hub' protein. *Nucleic acids research***39**, 6249-6259, doi:10.1093/nar/gkr176 (2011).

15 Liu, P. *et al.* Deficiency in a glutamine-specific methyltransferase for release factor causes mouse embryonic lethality. *Molecular and cellular biology***30**, 4245-4253, doi:10.1128/MCB.00218-10 (2010).

16 Kusevic, D., Kudithipudi, S. & Jeltsch, A. Substrate Specificity of the HEMK2 Protein Glutamine Methyltransferase and Identification of Novel Substrates. *The Journal of biological chemistry***291**, 6124-6133, doi:10.1074/jbc.M115.711952 (2016).

17 Woodcock, C. B., Yu, D., Zhang, X. & Cheng, X. Human HemK2/KMT9/N6AMT1 is an active protein methyltransferase, but does not act on DNA in vitro, in the presence of Trm112. *Cell discovery***5**, 50, doi:10.1038/s41421-019-0119-5 (2019).

18 Xiao, C. L. *et al.* N(6)-Methyladenine DNA Modification in the Human Genome. *Molecular cell***71**, 306-318 e307, doi:10.1016/j.molcel.2018.06.015 (2018).

19 Kummer, E. & Ban, N. Mechanisms and regulation of protein synthesis in mitochondria. *Nat Rev Mol Cell Biol***22**, 307-325, doi:10.1038/s41580-021-00332-2 (2021).

20 Richter, R. *et al.* A functional peptidyl-tRNA hydrolase, ICT1, has been recruited into the human mitochondrial ribosome. *The EMBO journal***29**, 1116-1125, doi:10.1038/emboj.2010.14 (2010).

21 Antonicka, H. *et al.* Mutations in C12orf65 in patients with encephalomyopathy and a mitochondrial translation defect. *American journal of human genetics***87**, 115-122, doi:10.1016/j.ajhg.2010.06.004 (2010).

22 Soleimanpour-Lichaei, H. R. *et al.* mtRF1a is a human mitochondrial translation release factor decoding the major termination codons UAA and UAG. *Molecular cell***27**, 745-757, doi:10.1016/j.molcel.2007.06.031 (2007).

23 Kummer, E., Schubert, K. N., Schoenhut, T., Scaiola, A. & Ban, N. Structural basis of translation termination, rescue, and recycling in mammalian mitochondria. *Molecular cell***81**, 2566-2582 e2566, doi:10.1016/j.molcel.2021.03.042 (2021).

24 Desai, N. *et al.* Elongational stalling activates mitoribosome-associated quality control. *Science***370**, 1105-1110, doi:10.1126/science.abc7782 (2020).

25 Hori, A., Yoshida, M., Shibata, T. & Ling, F. Reactive oxygen species regulate DNA copy number in isolated yeast mitochondria by triggering recombination-mediated replication. *Nucleic acids research***37**, 749-761, doi:10.1093/nar/gkn993 (2009).

26 Monteiro, L. B., Davanzo, G. G., de Aguiar, C. F. & Moraes-Vieira, P. M. M. Using flow cytometry for mitochondrial assays. *MethodsX***7**, 100938, doi:10.1016/j.mex.2020.100938 (2020).

27 Bogenhagen, D. F. & Haley, J. D. Pulse-chase SILAC-based analyses reveal selective oversynthesis and rapid turnover of mitochondrial protein components of respiratory complexes. *The Journal of biological chemistry***295**, 2544-2554, doi:10.1074/jbc.RA119.011791 (2020).

28 Zhang, X. *et al.* MicroRNA directly enhances mitochondrial translation during muscle differentiation. *Cell***158**, 607-619, doi:10.1016/j.cell.2014.05.047 (2014).

29 Yoon, B. C. *et al.* Local translation of extranuclear lamin B promotes axon maintenance. *Cell***148**, 752-764, doi:10.1016/j.cell.2011.11.064 (2012).

30 Mora, L., Heurgue-Hamard, V., de Zamaroczy, M., Kervestin, S. & Buckingham, R. H. Methylation of bacterial release factors RF1 and RF2 is required for normal translation termination in vivo. *The Journal of biological chemistry***282**, 35638-35645, doi:10.1074/jbc.M706076200 (2007).

31 Karczewski, K. J. *et al.* The mutational constraint spectrum quantified from variation in 141,456 humans. *Nature***581**, 434-443, doi:10.1038/s41586-020-2308-7 (2020).

32 Akabane, S., Ueda, T., Nierhaus, K. H. & Takeuchi, N. Ribosome rescue and translation termination at non-standard stop codons by ICT1 in mammalian mitochondria. *PLoS genetics***10**, e1004616, doi:10.1371/journal.pgen.1004616 (2014).

33 Chrzanowska-Lightowlers, Z. M. & Lightowlers, R. N. Response to "Ribosome Rescue and Translation Termination at Non-standard Stop Codons by ICT1 in Mammalian Mitochondria". *PLoS genetics***11**, e1005227, doi:10.1371/journal.pgen.1005227 (2015).

34 Takeuchi, N. & Nierhaus, K. H. Response to the Formal Letter of Z. Chrzanowska-Lightowlers and R. N. Lightowlers Regarding Our Article "Ribosome Rescue and Translation Termination at Non-Standard Stop Codons by ICT1 in Mammalian Mitochondria". *PLoS genetics***11**, e1005218, doi:10.1371/journal.pgen.1005218 (2015).

35 Greber, B. J. *et al.* Ribosome. The complete structure of the 55S mammalian mitochondrial ribosome. *Science***348**, 303-308, doi:10.1126/science.aaa3872 (2015).

36 Desai, N., Brown, A., Amunts, A. & Ramakrishnan, V. The structure of the yeast mitochondrial ribosome. *Science***355**, 528-531, doi:10.1126/science.aal2415 (2017).

37 El-Gebali, S. *et al.* The Pfam protein families database in 2019. *Nucleic acids research***47**, D427-D432, doi:10.1093/nar/gky995 (2019).

38 Crooks, G. E., Hon, G., Chandonia, J. M. & Brenner, S. E. WebLogo: a sequence logo generator. *Genome research***14**, 1188-1190, doi:10.1101/gr.849004 (2004).

39 Savojardo, C., Bruciaferri, N., Tartari, G., Martelli, P. L. & Casadio, R. DeepMito: accurate prediction of protein sub-mitochondrial localization using convolutional neural networks. *Bioinformatics***36**, 56-64, doi:10.1093/bioinformatics/btz512 (2020).

40 Fukasawa, Y. *et al.* MitoFates: improved prediction of mitochondrial targeting sequences and their cleavage sites. *Molecular & cellular proteomics : MCP***14**, 1113-1126, doi:10.1074/mcp.M114.043083 (2015).

41 Jones, D. T. & Cozzetto, D. DISOPRED3: precise disordered region predictions with annotated protein-binding activity. *Bioinformatics***31**, 857-863, doi:10.1093/bioinformatics/btu744 (2015).

42 Robert, X. & Gouet, P. Deciphering key features in protein structures with the new ENDscript server. *Nucleic acids research***42**, W320-324, doi:10.1093/nar/gku316 (2014).

43 Heckl, D. *et al.* Generation of mouse models of myeloid malignancy with combinatorial genetic lesions using CRISPR-Cas9 genome editing. *Nature biotechnology***32**, 941-946, doi:10.1038/nbt.2951 (2014).

44 Tzelepis, K. *et al.* A CRISPR Dropout Screen Identifies Genetic Vulnerabilities and Therapeutic Targets in Acute Myeloid Leukemia. *Cell reports***17**, 1193-1205, doi:10.1016/j.celrep.2016.09.079 (2016).

Figures

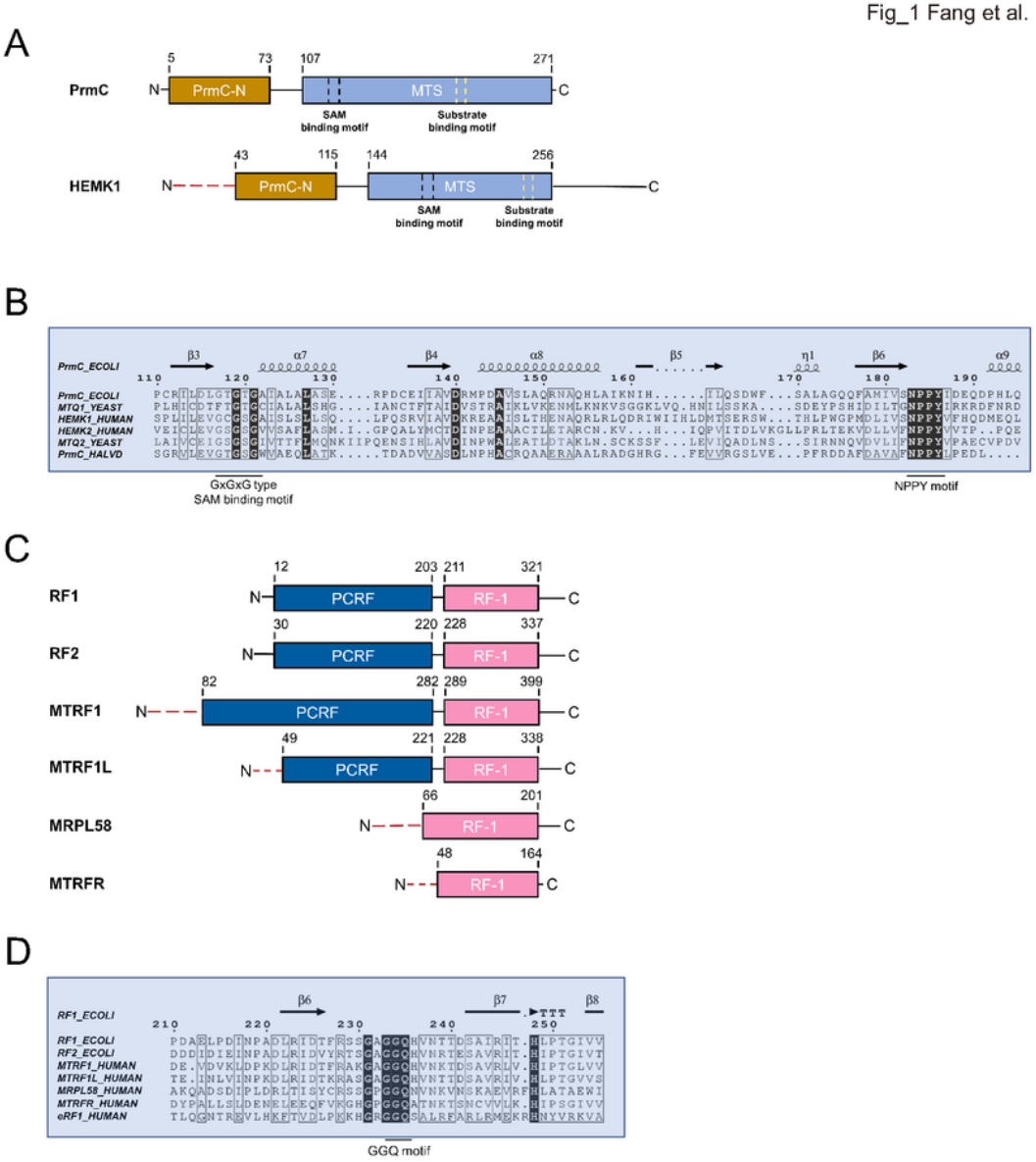

Figure 1

Domain architecture and sequence alignment of HEMK1 and mtRFs. A) Domain architecture of PrmC and HEMK1. B) Sequence alignments of various PrmC family proteins. The amino acid position is numbered according to the PrmC sequence. C) Domain architecture of bacterial RF1, RF2, and mtRFs. D) Sequence alignments of bacterial RF1, RF2, mtRFs, and the human eRF1. The amino acid position is numbered according to the bacterial RF1 sequence.

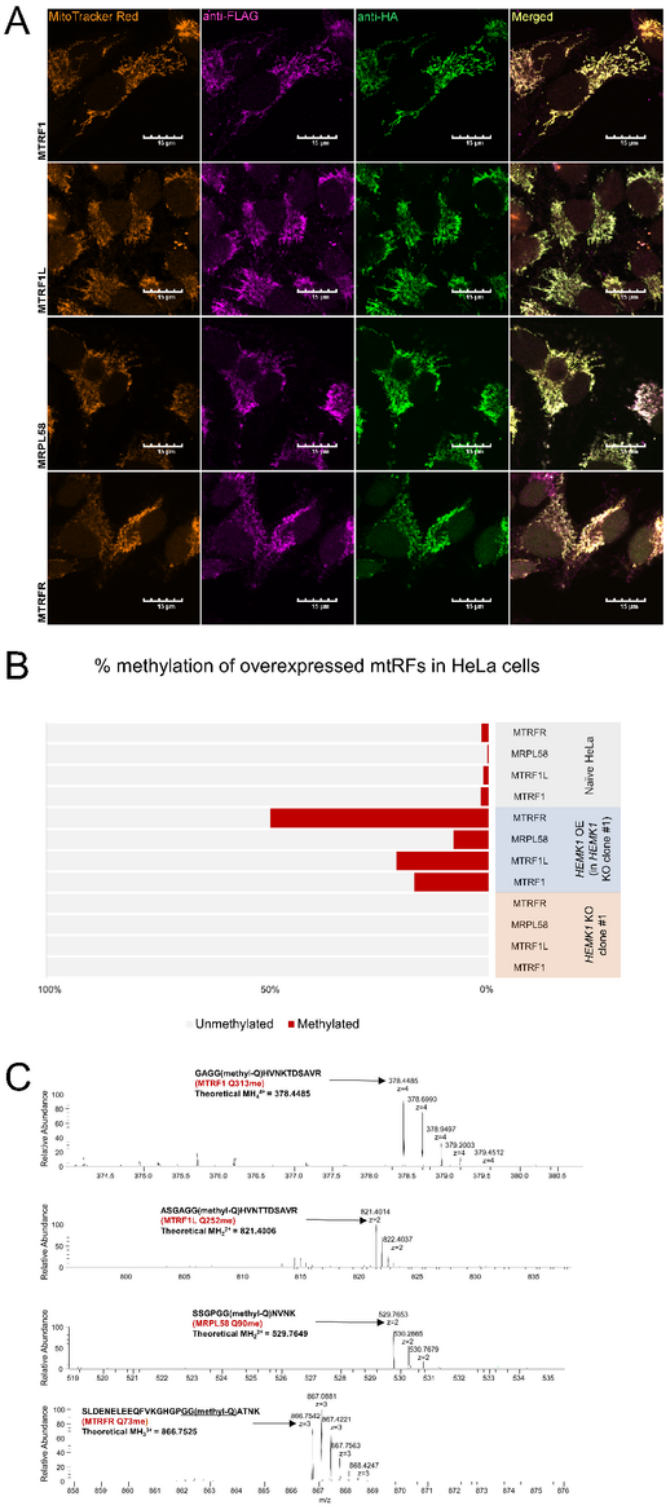

Figure 2

Glutamine methylation in the “GGQ” motif of four mtRFs mediated by HEMK1. A) Subcellular localization of stably expressed exogenous HEMK1 and mtRFs. HeLa cells expressed both HEMK1-cFLAG and individual mtRF-cHA were imaged. HEMK1-cFLAG, magenta; mtRFs-cHA, green; MitoTracker Red, orange. Scale: 15 μm. B) Methylation status of stably expressed exogenous mtRFs-cHA in naïve HeLa, HEMK1 KO clone #1, and HEMK1 KO clone #1 complemented with stably expressed HEMK1-cFlag. For fragment

counts and methylation ratio of each methylated peptide, see Figure S5A. C) MS1 spectra of mtRFs. Theoretical mass corresponds to specific methylated mtRFs peptides. See Figure S6A, and Table S2 for detailed MS2 spectra of methylation sites.

Fig_3 Fang et al.

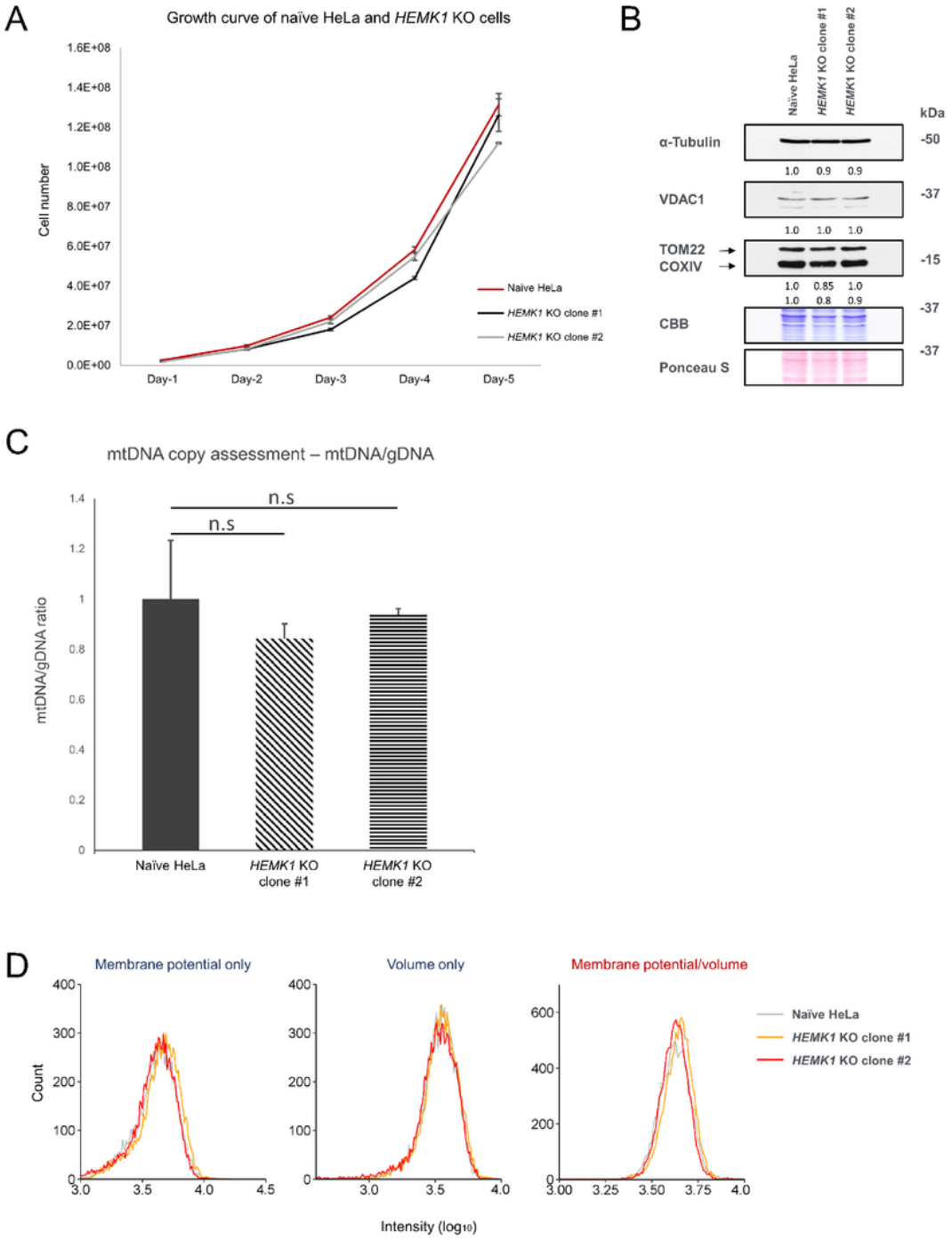

Figure 3

Impacts of HEMK1 depletion on cell growth and mitochondrial properties. A) Growth curve of naïve HeLa and HEMK1 KO clones #1 and #2. The numbers represent a mean ± SEM from three independent

samples. B) Western blot of mitochondrial outer membrane proteins VDAC1 and TOM22, and inner membrane protein COXIV from naïve HeLa and HEMK1 KO clones (#1 and #2). α-Tubulin was used as a loading control. CBB and Ponceau S staining were shown as loading and transfer indicators. Numbers shown at the bottom of each panel indicated the normalized intensity referring to signals from naïve HeLa. C) Assessment of relative mtDNA copy numbers by qPCR. Data were normalized to gDNA abundance. Data represent a mean ± SEM from three independent samples. A two-tailed test was used for statistical significance. n.s, not significant. D) Assessment of mitochondrial properties. The last panel represents the normalized mitochondrial membrane potential calculated from the membrane potential only and volume only panels (Membrane potential only/Volume only).

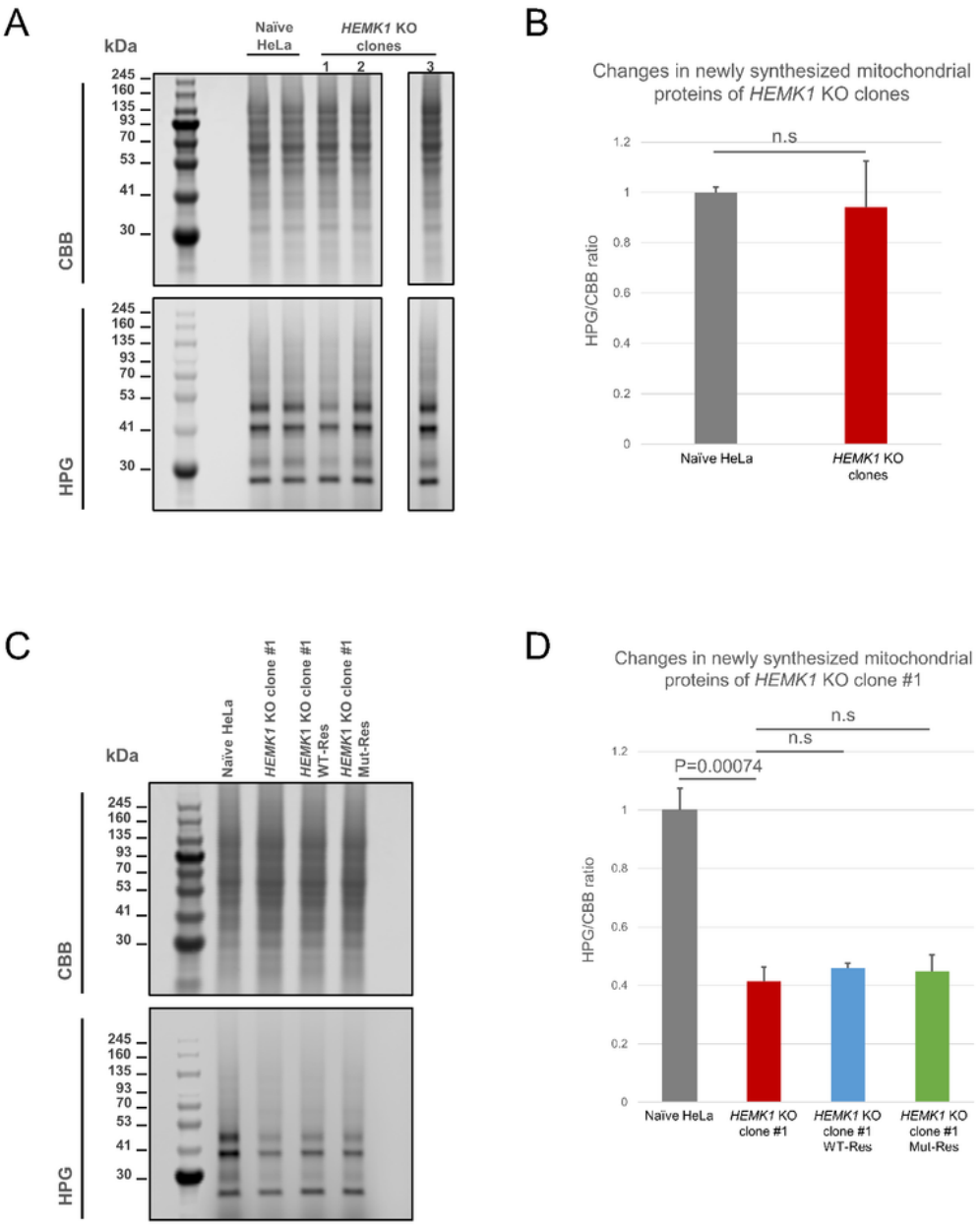

Figure 4

The assessment of mitochondrial translation in HEMK1 KO cells. A) Representative gel images of total and nascent mitochondrial proteins. Infrared (IR)-800 dye was conjugated to HPG-containing newly synthesized proteins. Total protein was stained with CBB. The space inserted between lanes 4 and 5 (counting from the left-hand side) because they were not adjacent lanes, although these lanes are originated from the same gel. The original image is shown in Figure S6A. B) Bar graph of HPG

signal/CBB signal for Figure 4A. Error bars represented the mean ± SEM calculated from samples shown in Figure S6A (see detailed measurements in Figure S6A). C) The same as A but wild-type HEMK1 [WT-res] or the mutant [Y242E] [Mut-res] was stably expressed in HEMK1 KO clone #1. D) Bar graph of HPG signal/CBB signal for Figure 4B. Error bars represented the mean ± SEM calculated from samples shown in Figure S6B (see detailed measurements in Figure S6B). A two-tailed t-test was used for statistical significance. n.s, not significant.

Supplementary Files

This is a list of supplementary files associated with this preprint. Click to download.

- HEMK1Suppfigandlegend.pdf
- TableS1.xlsx
- TableS2.xlsx